American Journal of Transplantation 2005; 5: 2170–2184
Blackwell Munksgaard

doi: 10.1111/j.1600-6143.2005.01026.x

Gene Expression Profiling in Murine Obliterative Airway Disease

Jeffrey D. Lande[a,b], Stacy L. Dalheimer[a,c], Daniel L. Mueller[a,c], Marshall I. Hertz[a,d] and Richard A. King[a,b,*]

[a] *Department of Medicine,* [b] *Institute of Human Genetics,* [c] *Center for Immunology and* [d] *Center for Advanced Lung Disease, University of Minnesota Medical School, Minneapolis, USA*
* *Corresponding author: Richard A. King, kingx002@umn.edu*

Lung and heart-lung transplantation are effective treatments for many diseases unresponsive to other therapy. However, long-term survival of recipients is limited by the development of obliterative bronchiolitis (OB). In this study, microarray analysis of a heterotopic mouse model of obliterative airway disease (OAD) was used to test the hypothesis that the expression and patterns of genes will correlate with specific changes in tracheal tissue developing a response to allotransplantation and the infiltrating cells manifesting these changes. Expression profiles observed were in accordance with the current paradigm of a predictable sequence of events, beginning with airway injury; an innate immune response followed by an adaptive immune response, including both cell-mediated and humoral components; and eventual loss of airway epithelial cells. These observations confirm and expand the list of genes and molecular processes that can be studied as potential surrogate markers or targets for intervention of OB.

Key words: Gene expression, lung transplantation, obliterative bronchiolitis, rejection

Received 22 March 2005, revised 7 May 2005 and accepted for publication 17 May 2005

Introduction

Lung and heart-lung transplantation are effective treatments for many diseases unresponsive to other therapy. However, long-term survival of recipients is often limited by the development of obliterative bronchiolitis (OB), a fibroproliferative condition affecting small airways (1–4). OB is generally thought to be a response to injury and inflammation resulting from acute vascular rejection, lymphocytic bronchiolitis, viral infections and other causes of bronchial injury (5). However, even as treatment for acute rejection and infection continue to improve, the incidence and severity of OB have not changed, resulting in graft and patient survival rates lower than those observed in other solid organ transplants (6,7).

Microarray analysis of gene expression has been performed with tissue from lung, kidney and heart transplant recipients in an attempt to learn more about the process of rejection (8–11). These studies have focused on acute rejection and have produced lists of genes that support the role of T-cell infiltration in grafted organs, and also indicate that there are different subprofiles of acute rejection.

The genome-wide screening capability of microarray analysis suggests the potential to identify new surrogate markers for OB and to better understand its underlying mechanisms. However, analysis of human samples is limited by heterogeneity among patients and an inability to obtain samples at specific stages in the development of the disease. To address these limitations, we performed microarray analysis of gene expression in a well-characterized murine model of obliterative airway disease (OAD) that reproduces characteristic features of OB (12). This is an attractive model because the evolution of the process is more rapid and the heterogeneity involved with human samples is avoided. We used this model system to test the hypothesis that there will be a sequential, stereotypic expression and patterns of genes that reflect pathophysiologic events in the grafts and in the graft-infiltrating cells.

Materials and Methods

Animal model

Male, 6–8-week-old wild-type BALB/c and C57BL/6 mice were purchased from the National Cancer Institute animal program of the NIH. BALB/c mice were used as tracheal graft donors into BALB/c recipients (isografts) or MHC incompatible C57BL/6 recipients (allografts), as described previously (Figure 1) (12). Four grafts were transplanted into a subcutaneous pocket in the back of each recipient to ensure an adequate yield of RNA. Based on prior publications, grafts were removed at day 4, 14 or 25 after transplantation to capture gene expression patterns (i) preceding adaptive immune response, (ii) during peak adaptive immune response and (iii) following peak adaptive immune response, but before grafts are expected to experience complete fibrosis, respectively (Figure 1) (13,14). As controls for normal tracheal expression, RNA was isolated from untransplanted BALB/c mouse tracheas.

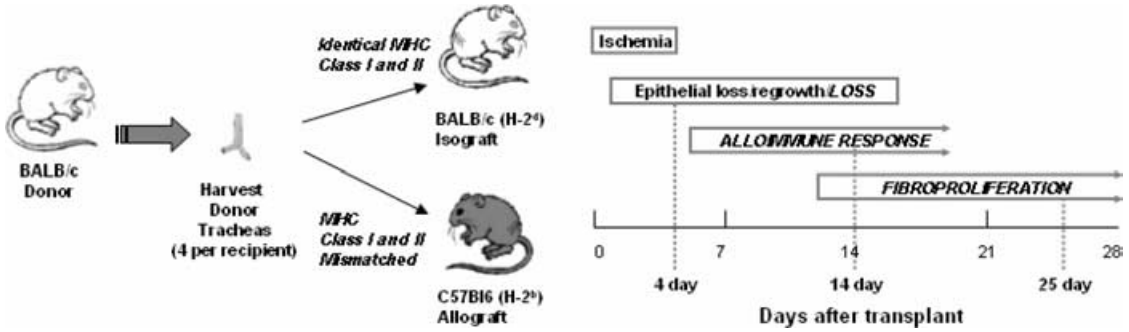

Figure 1: BALB/c mice were used as tracheal graft donors into MHC identical BALB/c recipients (isografts) or MHC incompatible C57BL/6 recipients (allografts). Four grafts were transplanted into a subcutaneous pocket in the back of each recipient and removed at day 4, 14 or 25 after transplantation. Continued epithelial loss, alloimmune response and fibroproliferation have been previously shown to be specific to the allograft recipients.

RNA isolation and microarray preparation

Tracheal grafts removed from the recipient mice were immediately immersed in RNALater (Qiagen, Valencia, CA). Grafts were placed in TRIzol (Invitrogen, Carlsbad, CA) and homogenized with Omni-Tips (Omni International, Marietta, GA) powered by a PowerGen 700 homogenizer (Fisher Scientific, Pittsburgh, PA). Homogenized grafts were further disrupted using a 19-gauge needle and total RNA was isolated using chloroform, isopropanol and ethanol (15). Isolated total RNA was suspended in RNase-free water and purified using the RNeasy kit (Qiagen Inc, Valencia, CA). RNA was discarded if the 260/280 ratio was not between 1.8 and 2.1, and RNA quality was assessed with the BioAnalyzer (Agilent Technologies, Palo Alto, CA).

A standard protocol was used to process total RNA for use with U430A murine GeneChips (Affymetrix, Santa Clara, CA). Using HPLC-purified T7-$(dT)_{24}$ primer, cDNA was synthesized from 10 μg of total RNA and transcribed into biotin-labeled cRNA using the Enzo in vitro transcription kit (Enzo Life Sciences, Farmingdale, NY). Biotin-labeled samples were then cleaned, fragmented and hybridized to GeneChips using the manufacturer's recommended methods (16).

Relationships and assumptions in data analysis

Numerous genes were represented multiple times on the GeneChip and many expressed sequence tags (ESTs) were also represented. For these reasons, we use the term transcript to refer to a GeneChip representation and the term gene when transcripts were mapped to genes using the LocusLink identifier (LL). Since different transcript representations of the same gene may have had different results in comparisons, it was necessary to make assumptions to summarize by LL. The approach we took was to consider a LL significant if any of the transcripts met the criteria for significance.

Data analysis

GeneChip data were analyzed using Microarray Suite version 5 (MAS5, Affymetrix), Gene Expressionist Refiner version 5.0 (GeneData, Basel, Switzerland) and Bioconductor within the R environment (version 2.0.1) (17). Transcripts were called present, marginal or absent using the MAS5 Detection algorithm. Chip quality was assessed using Refiner and only arrays that were of acceptable quality were used in the study. Transcript abundance was calculated within the Bioconductor GCRMA package (version 1.1.3), where background adjustment, normalization and condensing were performed. All statistical and visual data analysis was performed on expression estimates in log scale.

Transcripts with the highest amount of variation were defined by the coefficient of variation (CV; SD/mean). Genes with CV $\geq$ 0.5, which were called present on the majority of arrays ($\geq$3 out of 5) for at least one graft type and day combination (n = 3 554) were grouped by hierarchical two-dimensional clustering and principal components analysis.

Significance Analysis of Microarrays (SAM), implemented through the Bioconductor siggenes package (version 1.2.11), was used to find differentially expressed transcripts at each time point and for each of the six experimental conditions compared to normal tracheas (18). In each of the comparisons, a delta value was selected for an overall false discovery rate (FDR) <0.05.

Linear modeling was carried out on a per transcript basis within Bioconductor. For each probe set, the factDesign package (version 1.1.4) was used to compare a model including only graft day (number of days post-transplant −4, 14 or 25) to a model including graft day and graft type, as well as the interaction between those variables (19). Specifically, the linear model

$$\gamma_{ij} = \mu_i + \beta_{D14i} x_{D14j} + \beta_{D25i} x_{D25j} + \varepsilon_{ij}$$

was compared to the linear model

$$\gamma_{ij} = \mu_i + \beta_{14i} x_{14j} + \beta_{25i} x_{25j} + \beta_{Alloi} x_{Alloj} + \beta_{14:Alloi} x_{14:alloj} + \beta_{25:Alloi} x_{25:alloj} + \varepsilon_{ij}$$

separately for each gene i, where γ is the measure of transcript abundance (GCRMA), j refers to the sample, μ is the baseline value (a day 4 isograft in this arrangement), x is an indicator function for a given condition (e.g. for 14-day allografts, $x_{14} = 1$, $x_{25} = 0$ and $x_{Allo} = 1$), the β coefficients represent the day and graft type effects and ε represents random error.

The associated p-values for the F-test were adjusted for multiple comparison using the Benjamini and Hochberg correction that controls the FDR (20). Normal tracheas were not included in this comparison. Transcripts with an FDR <0.01 and that were present on the majority of arrays for at least one graft type and day combination were considered to be significant.

Analysis of the biological roles of sets of genes was performed using the GO and GOHyperG packages within the Bioconductor GOstats package (GOstats version 1.1.1, GO version 1.6.5 and moe430a version 1.6.5), taking advantage of data maintained by the Gene Ontology (GO) Consortium, which provide a dynamic vocabulary of three independent GO categories—molecular function (MF), biological process (BP) and cellular component (CC)—arranged into hierarchically nested nodes (21). LocusLink identifiers

and gene names were obtained in December 2004 from Affymetrix's NetAffx Analysis Center.

Two-dimensional hierarchical clustering was done using the Cluster and Treeview (version 1.60) applications (22). Within the cluster program, data were adjusted by centering across arrays by gene and the average linkage algorithm was used for clustering.

Principal components analysis and correlation of transcripts were accomplished using GeneData Expressionist Analyst version 5.0.6.

Quantitative RT-PCR

Quantitative RT-PCR was used to measure relative gene expression levels. One step RT-PCR was performed on an ABI Prism 7500 Real Time PCR System by using TaqMan 2 × Universal PCR master mix, 40X MultiScribe and RNase inhibitor mix and pre-optimized ABI Assays-on-Demand probes (Applied Biosystems, Foster City, Calif.) for interferon-γ and 18S rRNA using the manufacturer's recommended methods. Relative expression was estimated by the threshold cycle (C_T) of the gene of interest normalized to the C_T of 18S mRNA.

Results

Approach to data analysis

Gene expression studies with genome-wide representation generate a large amount of data, and the main difficulty is not in performing the experiment, but in interpreting the data in a biologically relevant manner. We have used several commonly used analytical strategies to test our hypothesis, and the following sections will provide details on each approach. Figure 2 represents the strategies employed. Summarization methods were utilized to narrow the initial data set to a smaller group of relevant transcripts. Cluster analysis and subsequent visualization provided insight into expression patterns. Classification methods were then used to test the hypothesis that there are stereotypic expression of genes and patterns of genes that reflect physiologic events.

Variation in gene expression between allografts and isografts

Two-dimensional cluster analysis was performed on the transcripts with the highest amount of variation across arrays to test the hypothesis that differences seen among arrays should be primarily due to the effects of the MHC mismatches. Isografts, allografts and normal tracheas were included in this analysis, but variation was calculated independently of class label. Three prominent clusters of arrays could be seen in the dendrogram (Figure 3). The first subcluster consisted of the 14- and 25-day isografts and normal tracheas. Allografts from days 14 and 25 exclusively made up the second subcluster. Day 4 grafts primarily made up the third cluster, although one of the day 25 isografts was also weakly linked to this cluster.

Due to the potential subjectivity of cluster analysis, an alternative approach was taken to determine if the same conclusion was reached (23). Principal components analysis was performed using these same transcripts, with similar results. Plotting the eigenvalues of the first three principal components in terms of experiments (Figure 4) suggested further distinction between 14- and 25-day allografts. Normal tracheas and 14/25-day isografts were slightly separated, as compared to the cluster analysis, but these groups still appeared more similar to each other than to 4-day grafts or 14/25-day allografts. These data indicate that differences between allografts and isografts were particularly pronounced at days 14 and 25, as predicted by the differences expected due to the adaptive immune response to MHC incompatibility. At day 4, before the adaptive immune response was expected to be fully engaged, allografts and isografts appear relatively similar in their overall expression.

Comparison of grafted and normal tracheas

All graft day and graft type combinations were compared pairwise to normal tracheas using SAM (Figure 5). Both isografts and allografts differed in expression of numerous transcripts at day 4 and continued to differ at day 14, although fewer transcripts differed in isografts. By day 25, there was a noticeable decrease in the number of transcripts different from normal tracheas in isografts, while the number remained relatively higher in allografts. These patterns suggest that following transplantation, isograft cells were able to regenerate and revert toward expression patterns indicative of normal tracheas, while cells in allografts were less able to redevelop.

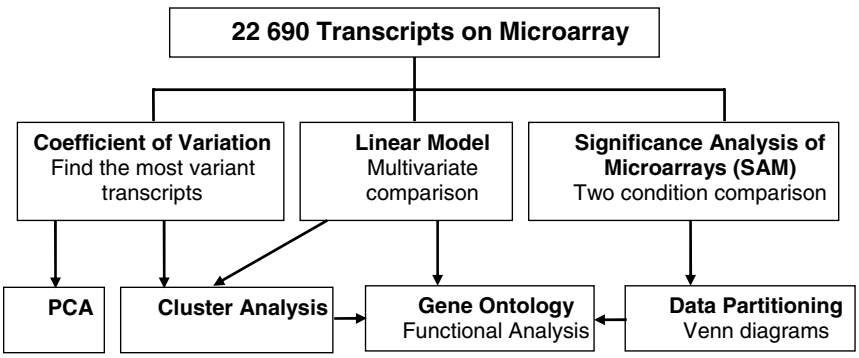

Figure 2: Coefficient of variation (CV), SAM analysis and linear modeling represent statistical summarization methods. These methods reduce the number of transcripts to those that are most relevant. CV allows limitation to the most variant transcripts and the other methods limit to transcripts that reflect the most significant pairwise group (SAM) or graft type group differences (LM). Cluster analysis, gene ontology, data partitioning and principal components analysis are methods then used to find patterns within and classify summarized data.

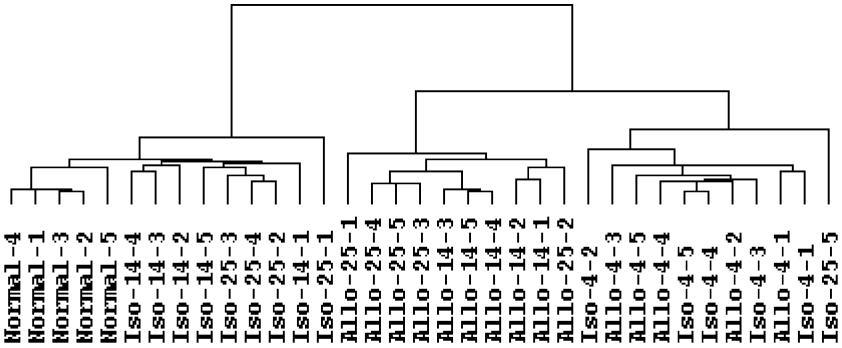

Figure 3: The dendrogram for the two-dimensional hierarchical cluster of the most variant genes (CV $>$ 0.5) on the microarray.

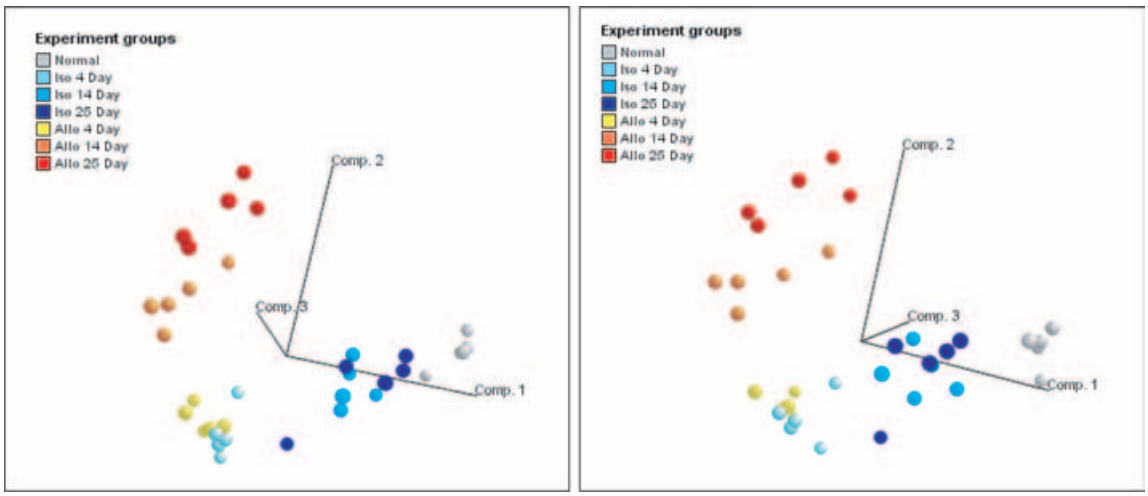

Figure 4: The first three principal components of the most variant genes on the microarray were plotted in three dimensions. Two different rotations of the three-dimensional plot are shown to better indicate the nature of the groupings.

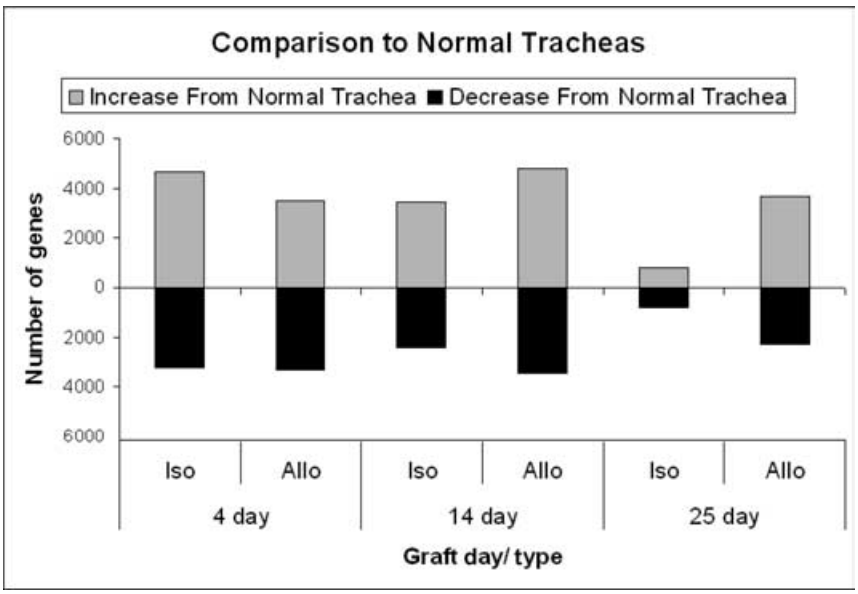

Figure 5: Comparisons were made between normal tracheas and each time point for allografts and isografts. For each condition, the number of significantly increased transcripts ($p < 0.05$) is shown in gray above the x-axis and the number of significantly decreased transcripts is shown in black below the x-axis.

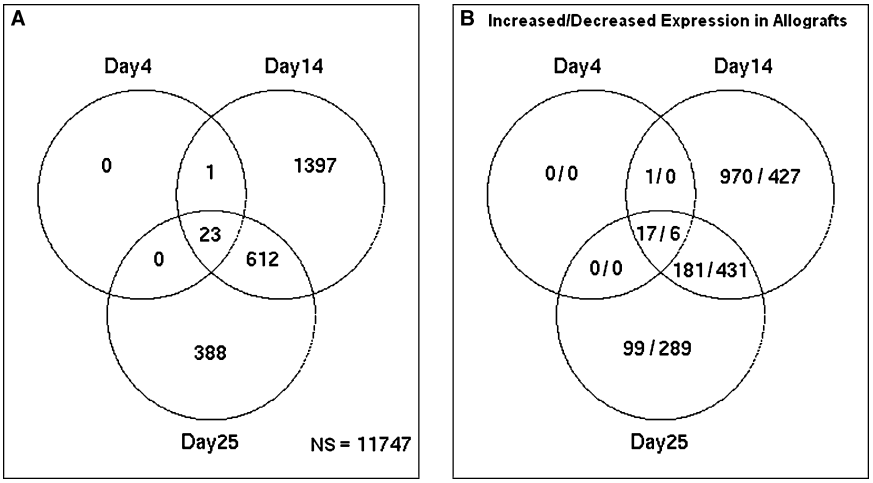

Figure 6: Significant expression differences ($p < 0.05$) between allografts and isografts are shown at days 4, 14 and 25, specified at the transcript level. (A) Circles in the Venn diagram correspond to differences at the specified day and overlapping regions indicate genes differentially expressed at all corresponding time points. For example, 23 transcripts were differentially expressed at day 4, 14 and 25. There were 11 747 transcripts that met the minimum criteria of present on the majority of arrays under any condition, but were not significant at any time point. (B) Venn diagrams were broken out by transcripts higher in allografts and lower in allografts.

Analysis of gene expression dynamics using data partitioning

In order to achieve a better perspective on the extent to which gene expression in allografts and isografts differed and whether expression differences in transcripts tended to be persistent in the three time points or unique to a particular time point, transcripts that showed a significant difference between graft types at each time point were arranged in a Venn diagram for data partitioning (Figure 6). There were few differences at day 4 compared to days 14 and 25 with only 23 transcripts showing a significant difference at all three time points and 1 at day 4 and 14 only (β2 integrin), indicating that differences seen at day 4 were generally persistent over the time points studied (Figure 6A). Table 1 lists the 24 transcripts and the fold change at each time point; a negative fold change indicates reduced expression in allografts and a positive fold change indicates increased expression in allografts. Histidine ammonia lyase and 5 MHC-associated proteins were relatively under-expressed in allografts, while STAT1, CXCL9, sorting nexin 6 and Pim-1 were among the transcripts increased in allografts at all three time points.

The number of transcripts expressed higher only in 14-day allografts (n = 970) exceeded the number of transcripts expressed higher at both day 14 and 25 (n = 181) or at day 25 only (n = 99), while the number of transcripts expressed at a lower level only in 14-day allografts (n = 427) was similar to those expressed lower at both day 14 and 25 (n = 431) and higher than those expressed higher only at day 25 (n = 289) (Figure 6B). This suggests a particularly active process, unique to day 14, possibly representative of the heavy T-cell infiltration known to occur around this time period (13). However, there were still substantial gene expression differences in common between days 14 and 25 and unique to day 25.

Characterization of 14- and 25-day grafts using gene ontology

To better understand the transcriptional differences at days 14 and 25, GO groupings (MF, BP and CC) were used to characterize the transcripts differentially expressed at days 14 and 25. For this analysis, we compared the GO nodes that were most overrepresented (hypergeometric p-value <0.001) by genes with higher expression in allografts at day 14 only (n = 810), day 25 only (n = 72) or at both time points (n = 166), or by genes with lower expression in allografts at day 14 only (n = 358), day 25 only (n = 248) or at both time points (n = 373). In the MF GO group, no nodes met the criteria for genes with lower expression in allografts, but 16 nodes showed higher expression in allografts in at least one of the three groups (Table 2 and Figure 7). Of these, cytoskeletal protein binding, actin binding and IgG binding were more overrepresented at day 14, MHC class I and II receptor activity were overrepresented at both days and day 25 did not have any nodes overrepresented at $p < 0.001$, although genes in the antigen binding node had a $p = 0.002$ (Table 2 and Figure 7B). The number of genes in the IgG binding and antigen binding groups was small, and these served as an example of how this type of analysis could be used at the different time points. All of the genes in the IgG binding group were Fc-receptor genes for binding IgG or IgE, while most of the significant genes in the antigen receptor group were structural immunoglobin genes (Table 3).

A similar analysis of the BP group showed high expression of genes related to cytokine production, biosynthesis and metabolism and DNA replication in day 14 allografts genes of the transmembrane receptor protein tyrosine kinase signaling pathway in day 25 allografts; and genes involved with T-cell selection and differentiation as well as antigen processing and presentation at both time points (supplemental data).

Table 1: Transcripts with significant expression differences at Day 4

		Fold change		
Affy ID	Gene description	Day 4	Day 14	Day 25
1422892_s_at	Histocompatibility 2, class II antigen E alpha	−67.82	−22.95	−34.66
1418645_at	Histidine ammonia lyase	−19.64	−8.67	−25.05
1422891_at	Histocompatibility 2, class II antigen E alpha	−4.00	−4.19	−4.00
1452544_x_at	Histocompatibility 2, D region locus 1	−2.82	−4.57	−21.60
1427651_x_at	Histocompatibility 2, D region///MHC (A.CA/J(H-2K-F) Class I antigen /// Histocompatibility 2, D region locus 1	−2.81	−3.82	−14.75
1425614_x_at	Histocompatibility 2, D region locus 1	−2.81	−4.06	−15.41
1450678_at	Integrin beta 2	1.62	2.32	
1436212_at	Expressed sequence AI661017	2.27	2.17	3.28
1449445_x_at	Microfibrillar-associated protein 1	2.73	6.28	6.27
1431008_at	RIKEN cDNA 0610037M15 gene	3.84	15.15	18.47
1460245_at	Killer cell lectin-like receptor, subfamily d, member 1	4.04	8.99	11.20
1455869_at	ESTs, moderately similar to A47643 hypothetical protein - mouse (fragment) [M.Musculus]	4.08	5.70	15.15
1424832_at	RIKEN cDNA 4732429D16 gene	4.10	3.42	6.12
1424987_at	RIKEN cDNA 5430435G22 gene	4.77	4.78	11.75
1450033_a_at	Signal transducer and activator of transcription 1	5.27	7.20	7.23
1434624_x_at	Ribosomal protein S9	5.48	13.44	12.95
1451602_at	Sorting nexin 6	6.52	7.36	4.10
1419043_a_at	Interferon-inducible GTPase	6.76	4.48	5.32
1424857_a_at	Tripartite motif protein 34	7.40	13.07	16.09
1452426_x_at	Unknown (blast - truncated pol/envelope fusion protein)	9.83	25.02	35.96
1435872_at	Proviral integration site 1	11.83	33.60	42.75
1418652_at	Chemokine (C-X-C motif) ligand 9	36.59	31.74	64.05
1421144_at	Retinitis pigmentosa GTPase regulator interacting protein 1	49.34	99.00	106.85
1435330_at	Expressed sequence AI447904 (IFN-inducible protein 203)	56.19	61.59	40.81

Table 2: Gene ontology – overrepresented molecular function at Days 14 and 25

			Higher Day 14 allo		Higher Day 25 allo		Higher Day 14/25 allo	
GO ID	Term	On Chip*	NGS**	p-Value	NGS**	p-value	NGS**	p-Value
GO:0005515	Protein binding	1834	160	<0.001	18	0.007	25	0.355
GO:0004871	Signal transducer activity	1595	125	0.012	13	0.092	39	<0.001
GO:0000166	Nucleotide binding	1096	103	<0.001	7	0.407	15	0.400
GO:0004872	Receptor activity	1090	91	0.007	11	0.034	33	<0.001
GO:0017076	Purine nucleotide binding	1083	102	<0.001	7	0.395	14	0.495
GO:0004888	Transmembrane receptor activity	577	41	0.300	5	0.214	22	<0.001
GO:0008092	Cytoskeletal protein binding	198	34	<0.001	1	0.672	1	0.920
GO:0003779	Actin binding	150	24	<0.001	1	0.569	1	0.852
GO:0019955	Cytokine binding	60	9	0.015	1	0.285	6	<0.001
GO:0001664	G-protein-coupled receptor binding	37	11	<0.001			2	0.078
GO:0042379	Chemokine receptor binding	35	11	<0.001			2	0.071
GO:0008009	Chemokine activity	35	11	<0.001			2	0.071
GO:0003823	Antigen binding	13			2	0.002	5	<0.001
GO:0045012	MHC class II receptor activity	8					7	<0.001
GO:0030106	MHC class I receptor activity	8	3	0.012			5	<0.001
GO:0019864	IgG binding	5	4	<0.001				

*On Chip refers to the number of genes represented on the microarray within that GO node.
**NGS is the number of genes significantly higher in allografts than isografts for each of the three groups.

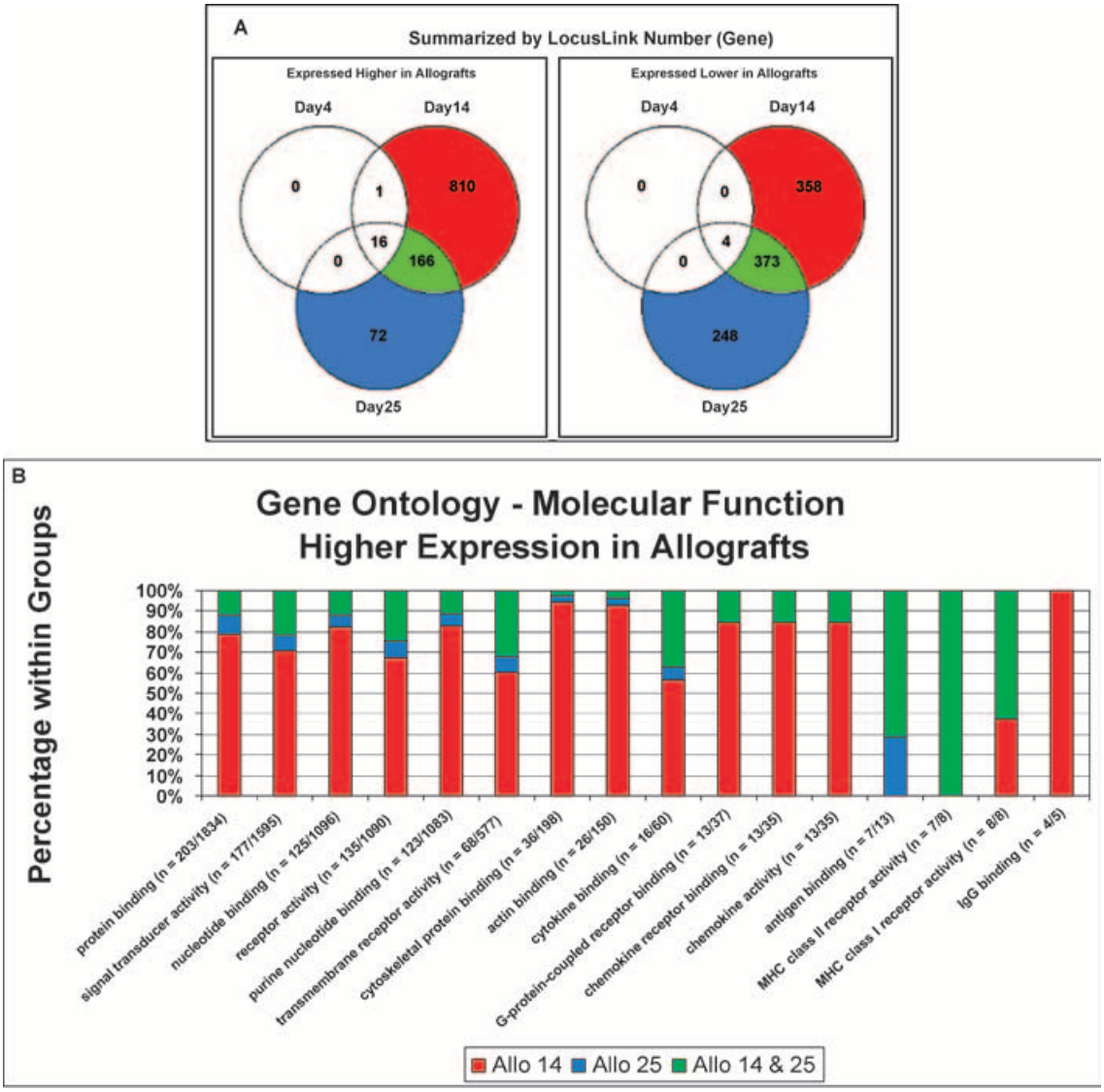

Figure 7: (A) Significant expression differences ($p < 0.05$) between allografts and isografts are shown at days 4, 14 and 25, specified at a gene level via the LL number and separated by increased and decreased expression in allografts. These Venn diagrams differ from that in Figure 6B, which was specified by transcript via the Affymetrix probe ID. To avoid ambiguities from multiple transcripts representing a LL number, if any of the transcripts were significant, the LL was considered significant. (B) A graphical representation of the data in Table 2, indicating the percentage of the overall number of genes represented within that node by each of the three time point groups. The numbers next to the gene ontology groups indicate the total number of genes significantly higher in allografts than isografts in the three time point groups and the total number of genes in that gene ontology node represented on the microarray.

The CC group analysis reinforced the overrepresentation of DNA replication genes at day 14, with 11 out of 27 spindle apparatus genes expressed higher in allografts. Immunological synapse and multi-vesicular body genes were CC categories overrepresented among those more highly expressed at days 14 and 25.

To this point, we have shown large scale differences in gene expression between isografts and allografts, particularly at days 14 and 25. The next series of analyses were performed to narrow down the transcripts of interest and to start explaining their biological relevance.

Genetic profile of obliterative airway disease

In order to create a parsimonious model that identified genes with a differential effect between allografts and isografts independent of the effect of time, a linear model

Table 3: IgG binding and antigen binding molecular function

IgG binding (GO: 0019864)			Fold change allo/iso		
LocusLink	Affy ID	Gene title	Day 4	Day 14	Day 25
14127	1418340_at	Fc receptor, IgE, high affinity I, gamma polypeptide		2.87	
14129	1417876_at	Fc receptor, IgG, high affinity I		6.89	
	1451941_a_at	Fc receptor, IgG, low affinity IIb		3.53	
14130	1435477_s_at	Fc receptor, IgG, low affinity IIb		3.02	
	1455332_x_at	Fc receptor, IgG, low affinity IIb		2.8	
	1435476_a_at	Fc receptor, IgG, low affinity IIb		1.79	
14131	1448620_at	Fc receptor, IgG, low affinity III		1.88	
14132	1416978_at	Fc receptor, IgG, alpha chain transporter			

IgG binding and antigen binding molecular function

Antigen binding (GO: 0003823)			Fold change allo/iso		
LocusLink	Affy ID	Gene title	Day 4	Day 14	Day 25
12507	1418353_at	CD5 antigen			3.08
14960	1435290_x_at	histocompatibility 2, class II antigen A, α		2.11	4.14
	1451721_a_at	histocompatibility 2, class II antigen A, β 1		2.89	4.6
14961	1450648_s_at	histocompatibility 2, class II antigen A, β 1		2.3	3.82
	1425477_x_at	histocompatibility 2, class II antigen A, β 1		2.2	
	1418734_at	histocompatibility 2, K1, K region			
15006	1420068_at	histocompatibility 2, Q region locus 1			
	1449720_at	histocompatibility 2, Q region locus 1			
15985	1417640_at	CD79B antigen			
	1425247_a_at	IgG heavy chain 4 (serum IgG1)			247.63
	1425324_x_at	IgG heavy chain 4 (serum IgG1)			72.27
	1427870_x_at	IgG heavy chain 4 (serum IgG1)			68.86
	1427756_x_at	IgG heavy chain 4 (serum IgG1)			39.24
16017	1426196_at	IgG heavy chain 4 (serum IgG1)			
	1427869_at	IgG heavy chain 4 (serum IgG1)			
	1427758_x_at	IgG heavy chain 4 (serum IgG1)			
	1452538_at	IgG heavy chain 4 (serum IgG1)			
	1455530_at	IgG heavy chain 6 (heavy chain of IgM)			
16019	1427351_s_at	IgG heavy chain 6 (heavy chain of IgM)		11.57	13.33
	1427329_a_at	IgG heavy chain 6 (heavy chain of IgM)		3.9	9.48
	1426198_at	IgG heavy chain 6 (heavy chain of IgM)			
	1426199_x_at	IgG heavy chain 6 (heavy chain of IgM)			
	1451958_at	IgG heavy chain 6 (heavy chain of IgM)			
16069	1424305_at	IgG joining chain			
16136	1420177_at	IgG lambda chain 5			
	1420176_x_at	IgG lambda chain 5			
	1430523_s_at	IgG lambda chain, variable 1		8.67	28.72
16142	1424931_s_at	IgG lambda chain, variable 1			19.62
	1427292_at	IgG lambda chain, variable 1			
50931	1449508_at	interleukin 27 receptor, alpha			
54167	1421931_at	inducible T-cell costimulator			
	1421930_at	inducible T-cell costimulator			
380793	1425385_a_at	IgG heavy chain 1a (serum IgG2a)		17.38	327.11
	1451632_a_at	Similar to IgG gamma-2a heavy chain			

including only the effect of day post-transplant was compared to a linear model that included the effect of day post-transplant in addition to type of graft and their interaction. Thus, any transcripts with significant changes in this analysis were due to the difference between graft types. Using this comparative linear model (CLM), 1677 transcripts were present on the majority of arrays for at least one of the six conditions and were significant after adjusting for multiple comparisons ($p < 0.01$).

Since there were no significantly different transcripts between graft types at day 4 only, the CLM was particularly helpful. The beta coefficients and corresponding p-values provide a summary of the overall effects of graft type and

the specific effects of graft type at day 14 and at day 25. Although there is one inestimable day/type interaction effect (4-day), there were no expected specific day 4 transcripts so this did not present a problem. The overall F-statistic can be used to generally rank transcripts within the model (supplemental data).

There were 2421 total transcripts significant in at least one of the three days by SAM analysis compared to only 1677 in the total linear model. Of the 1677 in the CLM, there were 146 transcripts that were not significant at any of the three times by SAM analysis, which appeared to be explained by the additional information provided by the overall variance calculated in the CLM (across all experimental conditions) compared to variance from bivariate analysis (between two conditions).

We also used two-dimensional hierarchical clustering again to visualize expression patterns among the CLM transcripts. Normal tracheas clustered with the 14- and 25-day isografts, but with less separation than in the cluster based on CV and there was not a clear differentiation between 14- and 25-day isografts. The remaining subclusters all clearly differentiated the remaining graft day and types. Clustering all 1677 CLM transcripts showed several prominent patterns of similar expression (Supplemental Figure 1). A large number of transcripts with low or no expression in normal tracheas had increased expression in both graft types at day 4 and reverted to pre-transplant levels at days 14 and 25. Profiling the genes and processes actively involved with the pathogenesis of OAD was of principal interest within this study, so we focused on clusters of transcripts with the most biological relevance, based on interpretation of expression patterns and previous knowledge of the heterotopic model.

Activated genes and processes in allografts

There was a small set of transcripts that stood out for their uniquely high-expression levels in day 14 allografts (Figure 8A). Genes with high day 14 expression included granzymes C and E, regenerating islet-derived 1, proprotein convertase subtilisin/kexin type 5, indoleamine-pyrrole 2,3 dioxygenase, ubiquitin D and IFN-γ and an EST. Flanking a set of transcripts with high expression at both day 14 and 25, including CD3, CD8 and T-cell receptor genes, were a set of transcripts that stood out for high levels of expression in 25-day allografts (Figure 8B). These transcripts were comprised principally of genes involved with humoral immune response. A cluster of genes with generally higher allograft expression included many genes that were found differentially expressed at all time points in the SAM analysis (Figure 8C).

Expression pattern reflective of epithelial loss

A cluster of transcripts showed a moderate decrease from normal tracheas in 4-day grafts that decreased noticeably in later allografts, but rose to the level of normal tracheas in later isografts. Several epithelial cell markers were among the transcripts in this cluster (supplemental Figure 2) and the most relevant gene ontology classifications of these genes by GO biological process were epithelial cell polarization and other processes associated with epithelial cell function, including establishment of epithelial cell polarity and morphogenesis, water and fluid transport and cell adhesion (Table 4).

Interferon gamma has a central and early role in rejection

At day 4, higher expression of transcripts associated with IFN-γ in allografts, such as STAT1 and CXCL9, implicated IFN-γ as being important in the process differentiating allografts from isografts (24, 25). However, although IFN-γ itself was expressed higher in allografts at a statistically significant level at day 14, it was not at day 4.

RT-PCR verification of the IFN-γ results was performed on three sets of the original samples and generally correlated well with the microarray results, although the RT-PCR data indicated there may have been relatively higher expression in allografts than suggested by microarray results at day 25 and, to a lesser extent, day 4 (Figure 9).

Transcripts with similarity to metalloproteinase-9

Metalloproteinase-9 (MMP-9), found among the 1677 CLM transcripts, has recently been strongly associated with OB in a porcine model (26). A list of transcripts correlating highly with MMP-9 across samples (correlation >0.75) was generated from our data set and found to be largely comprised of other genes within the CLM (32 of 51 transcripts) and contained several other genes that have been associated with fibrosis or OB, including ADAM12 and type V collagen (Table 5) (27,28).

Discussion

In this study, microarray analyses were used to show that gene expression dynamics at three distinct time points in a mouse model of chronic rejection were in accordance with the current paradigm of a predictable sequence of events, including an initial stage of ischemia-induced injury, reepithelialization and an innate immune response followed by an adaptive immune response, which included both cell-mediated and humoral components (13,29). Apparent from the expression profiles during the later time points was reduced expression in allografts of genes with epithelial cell function, consistent with the identification of airway epithelia as direct targets of allograft rejection (30,31). Our results also indicate the up-regulation of specific genes, including IFN-γ and MMP-9 that are known to be involved in alloimmunity and airway fibrosis.

A general problem of microarray-based experiments is selecting the appropriate analytical approach for very large

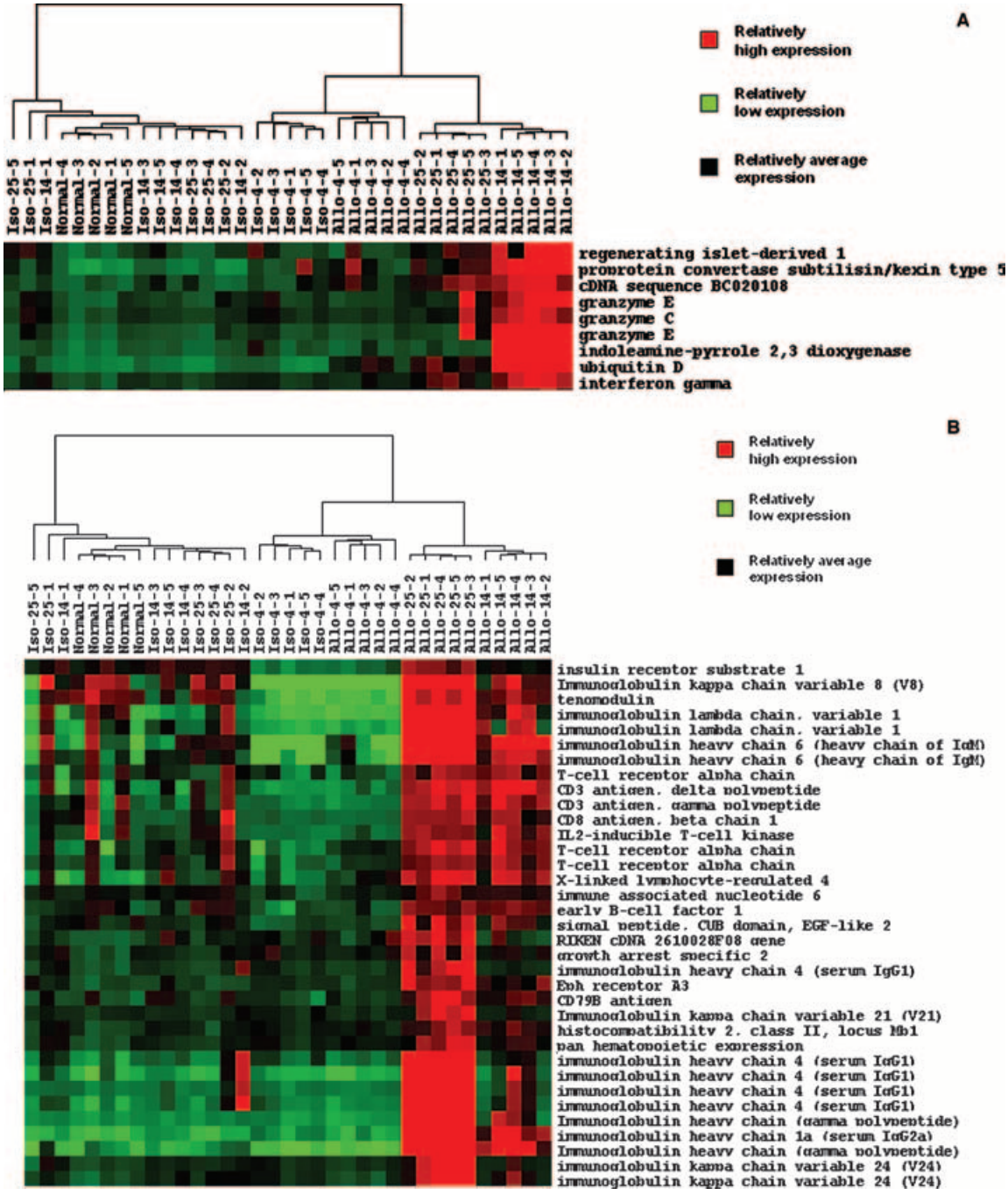

Figure 8: After two-dimensional hierarchical clustering of the 1677 transcripts significantly different between isografts and allografts ($p < 0.01$), clusters of transcripts with similar expression profiles were selected from the whole cluster of 1677, including one with uniquely high expression in (A) day 14 allografts, (B) day 25 allografts, and (C) all allograft time points.

data sets. Even given our simple experimental design, we found differences in gene expression patterns using different methodologies. In this case, inferences from multiple methodologies were made that would not have necessarily followed from any single methodology. As an example, we used multiple methods to analyze day 14 allografts. Individual comparison of time points with SAM followed by GO analysis was useful in finding a group of Fc-receptor genes with higher expression in 14-day allografts that was not apparent in the cluster analysis of the CLM results. Similarly, SAM analysis resulted in 970 transcripts with high 14-day expression, but cluster analysis of the CLM results

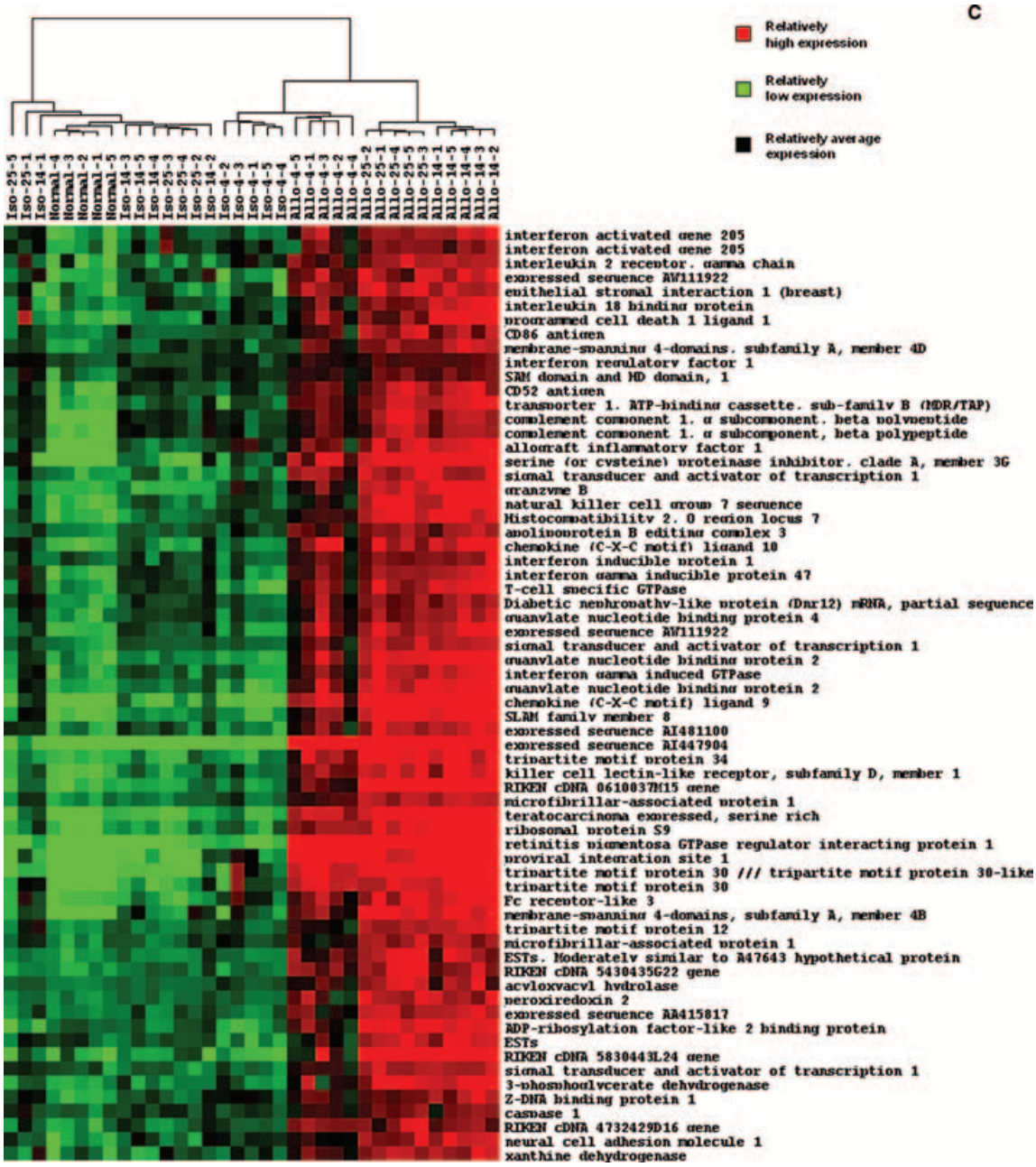

Figure 8: Continued.

revealed only a fairly small group of transcripts that stood out for particularly high expression. This emphasizes the importance of utilizing multiple complementary methodologies. All of these approaches provide useful information and each method has its strengths and weaknesses. GO analysis was extremely useful for finding patterns among large clusters of transcripts. In particular, GO was helpful for indicating that these clusters were often comprised of genes associated with a particular cell type or involved with a particular function. However, GO analysis was unable to find clusters of genes associated with fibrosis and fibroproliferation because these categories are not currently well populated into GO.

Prior studies have examined expression of specific genes in animal models of lung rejection. Using the mouse heterotopic model, Neuringer et al. showed IL-2, IL-4, IL-10, IFN-γ and granzyme B to be expressed higher in allografts (32). Likewise, a rat model of airway obliteration implicated similar genes, as well as MCP-1 and RANTES, which were

Table 4: Gene ontology – overrepresented biological process in 'epithelial loss' cluster

Biological process				
GO ID	Term	On Chip	NGS	p-Value
GO:0001736	Establishment of planar polarity	2	2	<0.001
GO:0007164	Establishment of tissue polarity	2	2	<0.001
GO:0001738	Morphogenesis of a polarized epithelium	2	4	<0.001
GO:0006833	Water transport	2	11	0.002
GO:0042044	Fluid transport	2	11	0.002
GO:0006116	NADH oxidation	1	1	0.007
GO:0042249	Establishment of polarity of embryonic epithelium	1	1	0.007
GO:0006734	NADH metabolism	1	1	0.007
GO:0007499	Ectoderm/mesoderm interaction	1	1	0.007
GO:0007185	Transmembrane receptor protein tyrosine phosphatase signaling pathway	2	19	0.007
GO:0007156	Homophilic cell adhesion	3	61	0.008

found to play an important role in the evolution of airway fibrosis (33,34). Transcripts representing IFN-γ, granzyme B, MCP-1 and RANTES were among the 1677 transcripts identified as significant in our study, while the three interleukins were not. General involvement of T-cell-associated cytokines and chemokines was indicated by GO analysis. Expected differences among interleukin genes may not have been apparent because of expression levels below the sensitivity level of the microarray or because those particular genes were not activated at the time points selected for study.

IFN-γ was previously associated with acute lung rejection (8) and was shown to be up-regulated in the identical heterotopic mouse model at 2 weeks and, to a lesser extent, at 4 weeks (32), consistent with the results in the current study. The profile induced in 4-day allografts in our study included IFN-γ-related transcripts, yet IFN-γ was not itself found in the profile. RT-PCR verification suggested a slight increase in day 4 allograft expression possibly below the sensitivity of the microarray. Further studies will be necessary to determine if IFN-γ was elevated transiently at another time point, thus leading to the induction of the associated genes whose expression was increased. Other possibilities were that the 'IFN-γ-associated' genes were induced by factors other than IFN-γ, or that IFN-γ underwent post-translational modifications that led to augmented downstream events in its targets.

Mouse trachea and human bronchioles are both populated by Clara cells (35). Clara cell secretory protein (CCSP, CC16, uteroglobin) was among the transcripts with significantly lower expression in day 14 and 25 allografts. CCSP has previously been shown to be expressed at a significantly lower level in human lung transplant recipients who eventually develop OB, consistent with their expression pattern in the current mouse study (36). This pattern suggests that Clara cells are either destroyed or functionally inactivated and emphasizes a potentially powerful aspect of the mouse model to provide insight into human OB.

Microarray technology allows us to expand our analysis beyond the set of genes already suspected to be involved with disease pathogenesis. For example, PLUNC, a secreted protein that has been shown to have anti-inflammatory properties, (37) had an expression pattern closely resembling that of CCSP, with a precipitous drop in expression in days 14 and 25 allografts. Regenerating islet-derived 1 expression resembled that of IFN-γ, with high expression in day 14 allografts. It has not been associated with lung allograft rejection in the past, but has been linked to chronic fibrotic pancreatitis (38). Further exploration of these and other genes with similar expression patterns is likely to yield insight into their roles in the pathogenic process.

The genome-wide screening ability of microarrays is particularly conducive to the study of OB, since the process is complex and successful intervention will likely require a more comprehensive study of the biology than single gene analysis will allow. Our study has begun to dissect the complexity of this process in a mouse model, offering both a comprehensive list of genes involved in the overall dynamics of the process and a strategy for further data analysis of this and similar datasets. Our findings will also serve as a baseline description of the gene expression dynamics, and will allow comparison with gene expression patterns in other experiments using this model of alloimmune-induced airway fibrosis.

Acknowledgments

This work was carried out in part using computing resources at the University of Minnesota Supercomputing Institute. In particular, Haoyu Yu provided support with installation and maintenance of UNIX-based Bioconductor packages. Initial RT-PCR optimization and data collection were done by Philip Jensen. The authors also thank Peter Bitterman for his ongoing support.

This study is supported by Lillehei Heart Institute, University of Minnesota and Institute of Human Genetics NIH Pulmonary Training Grant 5T32HL07741

First Group of verifications (correlation = -0.83381)

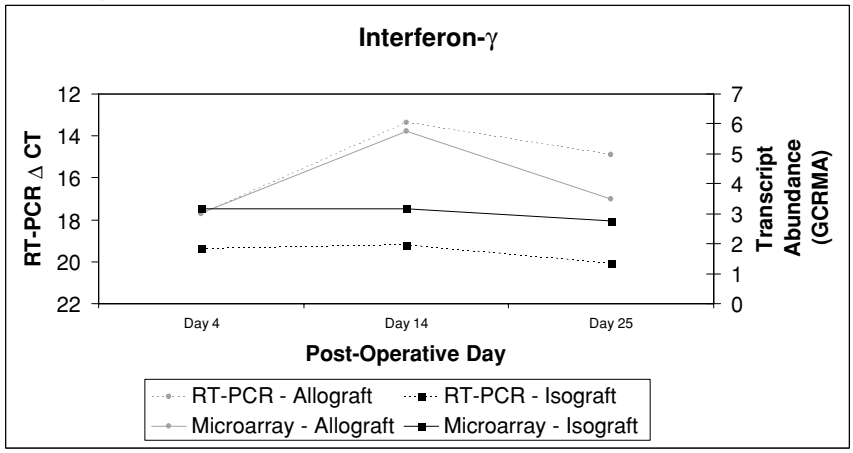

Second group (correlation = -0.6457)

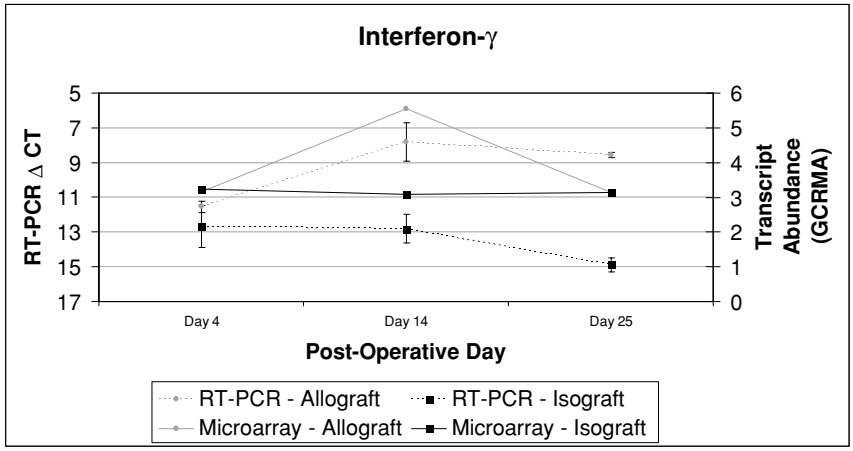

Third Group (correlation = -0.7469)

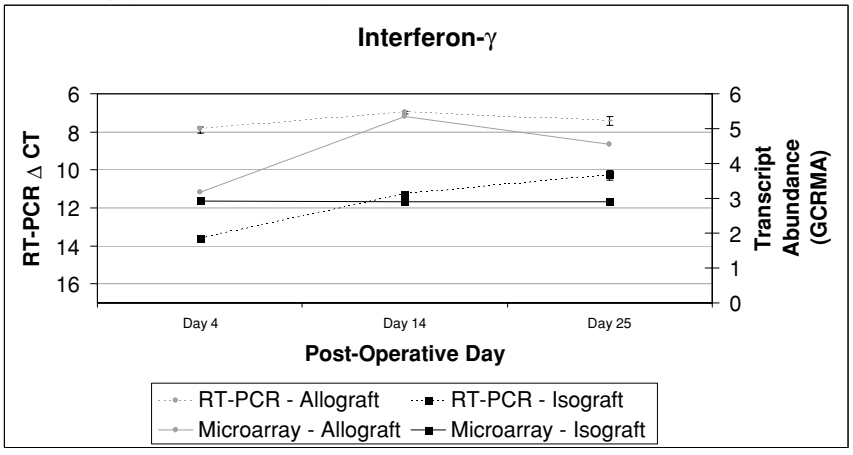

Figure 9: Three separate comparisons of samples used in the microarray analysis were verified using quantitative RT-PCR. RT-PCR data are measured in a scale that is inverse from that of the microarray data, so a high negative correlation implies agreement between the two measures.

Table 5: Transcripts with expression similarity to metalloproteinase 9

Probe set ID	Gene description	Correlation with MMP9
1416298_at	Matrix metalloproteinase 9	1
1448291_at	Matrix metalloproteinase 9	0.97
1421074_at	Cytochrome P450, 7b1	0.86
1415871_at	Transforming growth factor, beta induced, 68 kDa	0.83
1449632_s_at	FK506 binding protein 10	0.83
1421171_at	ADAM12 a disintegrin and metalloproteinase domain 12 (meltrin alpha)	0.83
1424650_at	Protein disulfide isomerase-related	0.83
1418269_at	Lysyl oxidase-like 3	0.83
1421268_at	UDP-glucose ceramide glucosyltransferase	0.82
1421075_s_at	Cytochrome P450, 7b1	0.82
1448123_s_at	Transforming growth factor, beta induced, 68 kDa	0.80
1426238_at	Bone morphogenetic protein 1	0.80
1421172_at	A disintegrin and metalloproteinase domain 12 (meltrin alpha)	0.79
1448378_at	Fascin homolog 1, actin bundling protein (Strongylocentrotus) purpuratus)	0.79
1424446_at	Armadillo repeat containing 7	0.79
1436512_at	ADP-ribosylation factor-like 7	0.79
1417291_at	Tumor necrosis factor receptor superfamily, member 1a	0.78
1417219_s_at	Thymosin, beta 10	0.78
1421694_a_at	Chondroitin sulfate proteoglycan 2	0.78
1456250_x_at	Transforming growth factor, beta induced, 68 kDa	0.78
1459903_at	Sema domain, immunoglobulin domain (Ig), and GPI membrane anchor, (semaphorin) 7A	0.78
1426955_at	Procollagen, type XVIII, alpha 1	0.78
1422507_at	Cystatin B	0.78
1449453_at	Bone marrow stromal cell antigen 1	0.78
1460205_at	RIKEN cDNA 6720485C15 gene	0.78
1460283_at	Mediterranean fever	0.78
1434479_at	Procollagen, type V, alpha 1	0.77
1450234_at	Membrane-spanning 4-domains, subfamily A, member 6C	0.77
1417836_at	Glutathione peroxidase 7	0.77
1448449_at	Receptor-interacting serine-threonine kinase 3	0.77
1417599_at	B7 homlog 3	0.77
1418547_at	Tissue factor pathway inhibitor 2	0.77
1418451_at	Guanine nucleotide binding protein (G protein), gamma 2 subunit	0.76
1452803_at	GLI pathogenesis-related 2	0.76
1416740_at	Procollagen, type V, alpha 1	0.76
1426239_s_at	Arrestin, beta 2	0.76
1420382_at	Apolipoprotein B48 receptor	0.76
1451406_a_at	Proprotein convertase subtilisin/kexin type 5	0.76
1418110_a_at	Inositol polyphosphate-5-phosphatase	0.76
1437889_x_at	Biglycan	0.76
1426909_at	Expressed sequence AI481316	0.76
1423407_a_at	Fibulin 2	0.76
1424086_at	RIKEN cDNA D130038B21 gene	0.76
1418074_at	Sialyltransferase 7 ((alpha-N-acetylneuraminyl 2,3-betagalactosyl-1,3)-N-acetyl galactosaminide alpha-2,6-sialyltransferase) D	0.76
1450826_a_at	Serum amyloid A 3	0.76
1423596_at	NIMA (never in mitosis gene a)-related expressed kinase 6	0.75
1416382_at	Cathepsin C	0.75
1431299_a_at	RIKEN cDNA 2310014H01 gene	0.75
1419598_at	Membrane-spanning 4-domains, subfamily A, member 6D	0.75
1436902_x_at	Thymosin, beta 10	0.75
1417277_at	Cytochrome P450, family 4, subfamily f, polypeptide 16	0.75

Transcripts in bold were in the 1677 transcripts from the CLM.

References

1. Arcasoy SM, Kotloff RM. Lung transplantation. N Engl J Med 1999; 340: 1081–1091.
2. Kelly KE, Hertz MI. Obliterative bronchiolitis. Clinics in Chest Medicine 1997; 18: 319–338.
3. Demeo DL, Ginns LC. Lung transplantation at the turn of the century. Annu Rev Med 200l; 52: 185–201.
4. Trulock EP Lung transplantation. Am J Respir Crit Care Med 1997; 155: 789–818.
5. Sharples LD, McNeil K, Stewart S, Wallwork J. Risk factors for bronchiolitis obliterans: a systematic review of recent publications. J Heart Lung Transplant 2002; 21: 271–281.
6. Boehler A, Estenne M. Post-transplant bronchiolitis obliterans. Eur Respir J. 2003; 22: 1007–1018.
7. Estenne M, Hertz MI. Bronchiolitis obliterans after human lung transplantation. Am J Respir Crit Care Med 2002; 166: 440–444.
8. Gimino VJ, Lande JD, Berryman TR, King RA, Hertz MI. Gene expression profiling of bronchoalveolar lavage cells in acute lung rejection. Am J Respir Crit Care Med 2003; 168: 1237–1242.
9. Sarwal M, Chua MS, Kambham N et al. Molecular heterogeneity in acute renal allograft rejection identified by DNA microarray profiling. N Engl J Med 2003; 349: 125–138.
10. Flechner SM, Kurian SM, Head SR et al. Kidney transplant rejection and tissue injury by gene profiling of biopsies and peripheral blood lymphocytes. Am J Transplant 2004; 4: 1475–1489.
11. Horwitz PA, Tsai EJ, Putt ME et al. Detection of cardiac allograft rejection and response to immunosuppressive therapy with peripheral blood gene expression. Circulation 2004; 110: 3815–3821.
12. Hertz MI, Jessurun J, King MB, Savik SK, Murray JJ. Reproduction of the obliterative bronchiolitis lesion after heterotopic transplantation of mouse airways. Am J Pathol 1993; 142: 1945–1951.
13. Kelly KE, Hertz MI, Mueller DL. Cell and major histocompatibility complex requirements for obliterative airway disease in heterotopically transplanted murine tracheas. Transplantation 1998; 66: 764–771.
14. Higuchi T, Jaramillo A, Kaleem Z, Patterson GA, Mohanakumar T. Different kinetics of obliterative airway disease development in heterotopic murine tracheal allografts induced by CD4 (+) and CD8 (+) T cells. Transplantation 2002; 74: 646–651.
15. Chomczynski P, Sacchi N. Single-step method of RNA isolation by acid guanidinium thiocyanate-phenol-chloroform extraction. Anal Biochem 1987; 162: 156–159.
16. Lockhart DJ, Dong HL, Byrne MC et al. Expression monitoring by hybridization to high-density oligonucleotide arrays. Nat Biotechnol 1996; 14: 1675–1680.
17. R Development Core Team. R: A language and Environment for Statistical Computing. 2004.
18. Tusher VG, Tibshirani R, Chu G. Significance analysis of microarrays applied to the ionizing radiation response. Proc Natl Acad Sci 2001; 98: 5116–5121.
19. Scholtens D, Miron A, Merchant M et al. Analyzing factorial designed microarray experiments. J Multivariate Anal 2004; 90: 19–43.
20. Benjamini Y, Hochberg Y. Controlling the false discovery rate—a practical and powerful approach to multiple testing. J R Stat Soc Ser B-Methodological 1995; 57: 289–300.
21. Ashburner M, Ball CA, Blake JA et al. Gene ontology: tool for the unification of biology. Nat Genet 2000; 25: 25–29.
22. Eisen MB, Spellman PT, Brown PO, Botstein D. Cluster analysis and display of genome-wide expression patterns. Proc Natl Acad Sci 1998; 95: 14863–14868.
23. Simon R, Radmacher MD, Dobbin K, McShane LM. Pitfalls in the use of DNA microarray data for diagnostic and prognostic classification. JNCI Cancer Spectr 2003; 95: 14–18.
24. Hiroi M, Ohmori Y. The transcriptional coactivator CREB-binding protein cooperates with STAT1 and NF-kappa B for synergistic transcriptional activation of the CXC ligand 9/Monokine induced by interferon-gamma Gene. J Biol Chem 2003; 278: 651–660.
25. Fulkerson PC, Zimmermann N, Hassman LM, Finkelman FD, Rothenberg ME. Pulmonary chemokine expression is coordinately regulated by STAT1, STAT6, and IFN-{gamma}. J Immunol 2004; 173: 7565–7574.
26. Eerola LM, Alho HS, Maasilta PK et al. Matrix metalloproteinase induction in post-transplant obliterative bronchiolitis. J Heart Lung Transplant 2005; 24: 426–432.
27. Sumpter TL, Wilkes DS. Role of autoimmunity in organ allograft rejection: a focus on immunity to type V collagen in the pathogenesis of lung transplant rejection. Am J Physiol Lung Cell Mol Physiol 2004; 286: L1129–L1139.
28. Skubitz KM, Skubitz APN. Gene expression in aggressive fibromatosis. J Lab Clin Med 2004; 143: 89–98.
29. Jaramillo A, Fernandez FG, Kuo EY, Trulock EP, Patterson GA, Mohanakumar T. Immune mechanisms in the pathogenesis of bronchiolitis obliterans syndrome after lung transplantation. Pediatr Transplant 2005; 9: 84–93.
30. Fernandez FG, Jaramillo A, Chen C et al. Airway epithelium is the primary target of allograft rejection in murine obliterative airway disease. Am J Transplant 2004; 4: 319–325.
31. Neuringer IP, Aris RM, Burns KA, Bartolotta TL, Chalermskulrat W, Randell SH. Epithelial kinetics in mouse heterotopic tracheal allografts. Am J Transplant 2002; 2: 410–419.
32. Neuringer IP, Walsh SP, Mannon RB, Gabriel S, Aris RM. Enhanced T cell cytokine gene expression in mouse airway obliterative bronchiolitis. Transplantation 2000; 69: 399–405.
33. Boehler A, Bai XH, Liu MY et al. Upregulation of T-helper 1 cytokines and chemokine expression in post-transplant airway obliteration. Am J Respir Crit Care Med 1999; 159: 1910–1917.
34. Suga M, MacLean AA, Keshavjee S, Fischer S, Moreira JMF, Liu MY. RANTES plays an important role in the evolution of allograft transplant-induced fibrous airway obliteration. Am J Respir Crit Care Med 2000; 162: 1940–1948.
35. Plopper CG Comparative morphologic features of bronchiolar epithelial cells. The Clara cell. Am Rev Respir Dis 1983; 128: S37–S41.
36. Nord M, Schubert K, Cassel TN, Andersson O, Riise GC. Decreased serum and bronchoalveolar lavage levels of Clara cell secretory protein (CC16) is associated with bronchiolitis obliterans syndrome and airway neutrophilia in lung transplant recipients. Transplantation 2002; 73: 1264–1269.
37. Geetha C, Venkatesh SG, Bingle L, Bingle CD, Gorr SU. Design and validation of anti-inflammatory peptides from human parotid secretory protein. J Dent Res 2005; 84: 149–153.
38. Bimmler D, Schiesser M, Perren A et al. Coordinate regulation of PSP/reg and PAP isoforms as a family of secretory stress proteins in an animal model of chronic pancreatitis. J Surg Res 2004; 118: 122–135.